LOCALIZED BASES FOR FINITE DIMENSIONAL HOMOGENIZATION APPROXIMATIONS WITH NON-SEPARATED SCALES AND HIGH-CONTRAST

HOUMAN OWHADI AND LEI ZHANG

Technical Report No. 2010-04
November 2010

APPLIED & COMPUTATIONAL MATHEMATICS
CALIFORNIA INSTITUTE OF TECHNOLOGY
mail code 217-50 · pasadena, ca 91125

Localized bases for finite dimensional homogenization approximations with non-separated scales and high-contrast.

Houman Owhadi[*], Lei Zhang[†]

November 3, 2010

Abstract

We construct finite-dimensional approximations of solution spaces of divergence form operators with L^∞-coefficients. Our method does not rely on concepts of ergodicity or scale-separation, but on the property that the solution of space of these operators is compactly embedded in H^1 if source terms are in the unit ball of L^2 instead of the unit ball of H^{-1}. Approximation spaces are generated by solving elliptic PDEs on localized sub-domains with source terms corresponding to approximation bases for H^2. The H^1-error estimates show that $\mathcal{O}(h^{-d})$-dimensional spaces with basis elements localized to sub-domains of diameter $\mathcal{O}(h^\alpha \ln \frac{1}{h})$ (with $\alpha \in [\frac{1}{2}, 1)$) result in an $\mathcal{O}(h^{2-2\alpha})$ accuracy for elliptic, parabolic and hyperbolic problems. For high-contrast media, the accuracy of the method is preserved provided that localized sub-domains contain buffer zones of width $\mathcal{O}(h^\alpha \ln \frac{1}{h})$ where the contrast of the medium remains bounded. The proposed method can naturally be generalized to vectorial equations (such as elasto-dynamics).

1 Introduction

Consider the partial differential equation

$$\begin{cases} -\operatorname{div}\Big(a(x)\nabla u(x)\Big) = g(x) \quad x \in \Omega;\ g \in L^2(\Omega),\ a(x) = \{a_{ij} \in L^\infty(\Omega)\} \\ u = 0 \quad \text{on} \quad \partial\Omega, \end{cases} \tag{1.1}$$

where Ω is a bounded subset of $\mathbb{R}^d$ with a smooth boundary (e.g., C^2) and a is symmetric and uniformly elliptic on Ω. It follows that the eigenvalues of a are uniformly bounded from below and above by two strictly positive constants, denoted by $\lambda_{\min}(a)$ and $\lambda_{\max}(a)$. Precisely, for all $\xi \in \mathbb{R}^d$ and $x \in \Omega$,

$$\lambda_{\min}(a)|\xi|^2 \le \xi^T a(x)\xi \le \lambda_{\max}(a)|\xi|^2. \tag{1.2}$$

[*]Corresponding author. California Institute of Technology, Computing & Mathematical Sciences , MC 217-50 Pasadena, CA 91125, owhadi@caltech.edu

[†]University of Oxford, Mathematical Institute

In this paper, we are interested in the homogenization of (1.1) (and its parabolic and hyperbolic analogues in Sections 4 and 5), but not in the classical sense, i.e. that of asymptotic analysis [8] or that of G or H-convergence ([41], [49, 27]) in which one considers a sequence of operators $-\operatorname{div}(a_\epsilon \nabla)$ and seeks to characterize limits of solution. We are interested in the homogenization of (1.1) in the sense of "numerical homogenization," i.e. that of the approximation of the solution space of (1.1) by a finite-dimensional space.

This approximation is not based on concepts of scale separation and/or of ergodicity but on compactness properties, i.e. the fact that the unit ball of the solution space is compactly embedded into $H^1_0(\Omega)$ if source terms (g) are integrable enough. This higher integrability condition on g is necessary because if g spans $H^{-1}(\Omega)$, then the solution space of (1.1) is $H^1_0(\Omega)$ (and it is not possible to obtain a finite dimensional approximation subspace of $H^1_0(\Omega)$ with arbitrary accuracy in H^1-norm). However, if g spans the unit ball of $L^2(\Omega)$, then the solution space of (1.1) shrinks to a compact subset of $H^1_0(\Omega)$ that can be approximated to an arbitrary accuracy in H^1-norm by finite-dimensional spaces [9] (observe that if $a = I_d$, then the solution space is a closed bounded subset of $H^2 \cap H^1_0(\Omega)$, which is known to be compactly embedded into $H^1_0(\Omega)$).

The identification of localized bases spanning accurate approximation spaces relies on a transfer property obtained in [9]. For the sake of completeness, we will give a short reminder of that property in Section 2. In Section 3, we will construct localized approximation bases with rigorous error estimates (under no further assumptions on a than those given above). In Sub-section 3.4, we will also address the high-contrast scenario in which $\lambda_{\max}(a)$ is allowed to be large. In Sections 4 and 5, we will show that the approximation spaces obtained by solving localized elliptic PDEs remain accurate for parabolic and hyperbolic time-dependent problems. We refer to Sub-section 6.2 for numerical experiments.

2 A reminder on the flux-norm and the transfer property.

Recall that the key element in G and H convergence is a notion of "compactness by compensation" combined with convergence of fluxes. Here, the notion of compactness is combined with a flux-norm introduced in [9].

The flux-norm.

Definition 2.1. For $k \in (L^2(\Omega))^d$, denote by k_{pot} the potential portion of the Weyl-Helmholtz decomposition of k. Recall that k_{pot} is the orthogonal projection of k onto $\{\nabla f \,:\, f \in H^1_0\Omega)\}$ in $(L^2(\Omega))^d$.

Definition 2.2. For $\psi \in H^1_0(\Omega)$, define

$$\|\psi\|_{a\text{-flux}} := \|(a\nabla\psi)_{pot}\|_{(L^2(\Omega))^d}. \tag{2.1}$$

We call $\|\psi\|_{a\text{-flux}}$ the flux-norm of Ψ.

The following proposition shows that the flux-norm is equivalent to the energy norm if $\lambda_{\min}(a) > 0$ and $\lambda_{\min}(a) < \infty$.

Proposition 2.1. [Proposition 2.1 of [9]] $\|.\|_{a\text{-flux}}$ *is a norm on* $H^1_0(\Omega)$. *Furthermore, for all* $\psi \in H^1_0(\Omega)$

$$\lambda_{\min}(a)\|\nabla\psi\|_{(L^2(\Omega))^d} \leq \|\psi\|_{a\text{-flux}} \leq \lambda_{\max}(a)\|\nabla\psi\|_{(L^2(\Omega))^d} \tag{2.2}$$

Motivations behind the flux-norm: There are three main motivations behind the introduction of the flux norm.

- The flux-norm allows to obtain approximation error estimates independent from both the minimum and maximum eigenvalues of a. In fact, the flux-norm of the solution of (1.1) is independent from a altogether since

$$\|u\|_{a\text{-flux}} = \|\nabla\Delta^{-1}g\|_{(L^2(\Omega))^d} \tag{2.3}$$

- The $(\cdot)_{\text{pot}}$ in the a-flux-norm is explained by the fact that in practice, we are interested in fluxes (of heat, stress, oil, pollutant) entering or exiting a given domain. Furthermore, for a vector field ξ, $\int_{\partial\Omega} \xi \cdot n ds = \int_\Omega \operatorname{div}(\xi_{\text{pot}})dx$, which means that the flux entering or exiting is determined by the potential part of the vector field.

- Classical homogenization is associated with two types of convergence: convergence of energies (Γ-convergence [28, 13]) and convergence of fluxes (G or H-convergence [41, 27, 50, 49, 40]). Similarly, one can define an energy norm and a flux-norm.

The transfer property. For V, a finite dimensional linear subspace of $H^1_0(\Omega)$, we define

$$(\operatorname{div} a\nabla V) := \operatorname{span}\{\operatorname{div}(a\nabla v) \,:\, v \in V\}. \tag{2.4}$$

Note that $(\operatorname{div} a\nabla V)$ is a finite dimensional subspace of $H^{-1}(\Omega)$.

Theorem 2.1. (Transfer property of the flux norm) [Theorem 2.1 of [9]] *Let* V' *and* V *be finite-dimensional subspaces of* $H^1_0(\Omega)$. *For* $f \in L^2(\Omega)$, *let* u *be the solution of (1.1) with conductivity* a *and* u' *be the solution of (1.1) with conductivity* a'. *If* $(\operatorname{div} a\nabla V) = (\operatorname{div} a'\nabla V')$, *then*

$$\inf_{v\in V} \frac{\|u-v\|_{a\text{-flux}}}{\|g\|_{L^2(\Omega)}} = \inf_{v\in V'} \frac{\|u'-v\|_{a'\text{-flux}}}{\|g\|_{L^2(\Omega)}}. \tag{2.5}$$

The usefulness of (2.5) can be illustrated by considering $a' = I$ so that $\operatorname{div} a'\nabla = \Delta$. Then, $u' \in H^2$ and therefore V' can be chosen as, e.g., the standard piecewise linear FEM space, on a regular triangulation of Ω of resolution h, with nodal basis $\{\phi_i\}$. The space V is then defined by its basis $\{\theta_i\}$ determined by

$$\begin{cases} \operatorname{div}(a\nabla\theta_i) = \Delta\phi_i & \text{in} \quad \Omega \\ \theta_i = 0 & \text{on} \quad \partial\Omega \end{cases} \tag{2.6}$$

Equation (2.5) shows that the approximation error estimate associated with the space V and the problem with arbitrarily rough coefficients is (in a-flux norm) equal to the approximation error estimate associated with piecewise linear elements and the space $H^2(\Omega)$. More precisely,

$$\sup_{g \in L^2(\Omega)} \inf_{v \in V} \frac{\|u - v\|_{a\text{-flux}}}{\|g\|_{L^2(\Omega)}} \leq Ch \tag{2.7}$$

where C does not depend on a.

We refer to [17], [20] and [10] for recent results on finite element methods for high contrast ($\lambda_{\max}(a)/\lambda_{\min}(a) >> 1$) but non-degenerate ($\lambda_{\min}(a) = \mathcal{O}(1)$) media under specific assumptions on the morphology of the (high-contrast) inclusions (in [17], the mesh has to be adapted to the morphology of the inclusions). Observe that the proposed method remains accurate if the medium is both of high contrast and degenerate ($\lambda_{\min}(a) << 1$), without any further limitations on a, at the cost of solving PDEs (2.6) over the whole domain Ω.

Remark 2.1. We refer to [9] for the optimal constant C in (2.7). This question of optimal approximation with respect to a linear finite dimensional space is related to the Kolmogorov n-width [47, 38], which measures how accurately a given set of functions can be approximated by linear spaces of dimension n in a given norm. A surprising result of the theory of n-widths is the non-uniqueness of the space realizing the optimal approximation [47].

3 Localization of the transfer property.

The elliptic PDEs (2.6) have to be solved on the whole domain Ω. Is it possible to localize the computation of the basis elements θ_i to a neighborhood of the support of the elements ϕ_i? Observe that the support of each ϕ_i is contained in a ball $B(x_i, C\,h)$ of center x_i (the node of the coarse mesh associated with x_i) of radius $C\,h$. Let $0 < \alpha \leq 1$. Solving the PDEs (2.6) on sub-domains of Ω (containing the support of ϕ_i) may, a priori, increase the error estimate in the right hand side of (2.5). This increase can, in fact, be linked to the decay of the Green's function of the operator $-\operatorname{div}(a\nabla)$. The slower the decay, the larger the degradation of those approximation error estimates. Inspired by the strategy used in [30] for controlling cell resonance errors in the computation of the effective conductivity of periodic or stochastic homogenization (see also [31, 46, 54]), we will replace the operator $-\operatorname{div}(a\nabla)$ by the operator $\frac{1}{T} - \operatorname{div}(a\nabla)$ in the left hand side of (2.6) in order to artificially introduce an exponential decay in the Green's function. A fine tuning of T is required because although a decrease in T improves the decay of the Green function, it also deteriorates the accuracy of the transfer property. In order to limit this deterioration, we will transfer a vector space with a higher approximation order than the one associated with piecewise linear elements. Let us now give the main result.

3.1 Localized bases functions.

Let $h \in (0,1)$. Let X_h be an approximation sub-vector space of $H^1_0(\Omega)$ such that

- X_h is spanned by basis functions $(\varphi_i)_{1\leq i\leq N}$ (with $N=\mathcal{O}(|\Omega|/h^d)$) with supports in $B(x_i, C\,h)$ where, the x_i are the nodes of a regular triangulation of Ω of resolution h.

- X_h satisfies the following approximation properties: For all $f \in H^1_0(\Omega)\cap H^2(\Omega)$

$$\inf_{v\in X_h} \|f-v\|_{H^1_0(\Omega)} \leq C\,h\|f\|_{H^2(\Omega)} \tag{3.1}$$

  and for all $f \in H^1_0(\Omega)\cap H^3(\Omega)$

$$\inf_{v\in X_h} \|f-v\|_{H^1_0(\Omega)} \leq C\,h^2\|f\|_{H^3(\Omega)} \tag{3.2}$$

- For all i,

$$\int_\Omega |\nabla \varphi_i|^2 \leq C h^{d-2} \tag{3.3}$$

- For all coefficients c_i,

$$h^d \sum_i c_i^2 \leq C\|\sum_i c_i\varphi_i\|^2_{L^2(\Omega)} \tag{3.4}$$

Examples of such spaces can be found in [15] and constructed using piecewise quadratic polynomials. Through this paper, we will write C any constant that does not depend on h (but may depend on d, Ω, and the essential supremum and infimum of the maximum and minimum eigenvalues of a over Ω). Let $\alpha \in (0,1)$ and $C_1>0$. For each basis element φ_i of X_h let ψ_i be the solution of

$$\begin{cases} h^{-2\alpha}\psi_i - \operatorname{div}(a\nabla\psi_i) = \Delta\varphi_i & \text{in} \quad B(x_i, C_1 h^\alpha \ln\frac{1}{h})\cap\Omega \\ \psi_i = 0 & \text{on} \quad \partial\big(B(x_i, C_1 h^\alpha \ln\frac{1}{h})\cap\Omega\big) \end{cases} \tag{3.5}$$

Let

$$V_h := \operatorname{span}(\psi_i) \tag{3.6}$$

be the linear space spanned by the elements ψ_i.

Theorem 3.1. *For $g \in L^2(\Omega)$, let u be the solution of (1.1) in $H^1_0(\Omega)$ and u_h the solution of (1.1) in V_h. There exists $C_0>0$ such that for $C_1 \geq C_0$, we have*

$$\frac{\|u-u_h\|_{H^1_0(\Omega)}}{\|g\|_{L^2(\Omega)}} \leq \begin{cases} Ch & \text{if} \quad \alpha\in(0,\frac{1}{2}] \\ Ch^{2-2\alpha} & \text{if} \quad \alpha \in [\frac{1}{2},1) \end{cases} \tag{3.7}$$

where the constants C and C_0 depend on a, d, Ω but not on h.

Remark 3.1. Theorem 3.1 shows the convergence rate in approximation error remains optimal (i.e. proportional to h) after localization if $0 < \alpha \leq 1/2$ and decays to 0 as $h^{2-2\alpha}$ for $\frac{1}{2} \leq \alpha < 1$. In particular, choosing localized domains with radii $\mathcal{O}(\sqrt{h}\ln\frac{1}{h})$ is sufficient to obtain the optimal convergence rate $\mathcal{O}(h)$.

Remark 3.2. It is possible to give an explicit value for C_0 by tracking constants in the proof.

Remark 3.3. If one uses piecewise linear basis elements instead of the elements φ_i (i.e. in the absence of property (3.2)), then the estimate in the right hand side of (3.7) deteriorates to $h^{1-2\alpha}$.

Remark 3.4. One could use piecewise linear basis elements instead of the elements φ_i, and also remove the term $h^{-2\alpha}\psi_i$ from the transfer property (3.5). In this situation, we numerically observe a rate of convergence of h for periodic, stochastic and low-contrast media after localization of (3.5) to balls of radii $\mathcal{O}(h)$. In these *particular* situations (characterized by short range correlations in a), the term $h^{-2\alpha}\psi_i$ should be avoided to obtain the optimal convergence rate h after localization to sub-domains of size $\mathcal{O}(h)$. In that sense, the estimate in the right hand side of (3.7) corresponds to a *worst case scenario* with respect to the medium a (characterized by long range correlations), requiring the introduction of the term $h^{-1}\psi_i$ and a localization to sub-domains of size $\mathcal{O}(\sqrt{h}\ln\frac{1}{h})$ for the optimal convergence rate h.

Remark 3.5. For the elliptic problem, computational gains result from localization (the elements ψ_i are computed on sub-domains Ω_i of Ω), parallelization (the elements ψ_i can be computed independently from each other), and the fact that the same basis can be used for different right hand sides g in (1.1). Computational gains are even more significant for time-dependent problems because, once an accurate basis has been determined for the elliptic problem, the same basis can be used for the associated (parabolic and hyperbolic) time-dependent problems with the same accuracy (we refer to Sections 4 and 5). For the wave equation with rough bulk modulus and density coefficients, the proposed method (based on pre-computing basis elements as solutions of localized elliptic PDEs) remains accurate, provided that high frequencies are not strongly excited ($\partial_t g \in L^2$).

On Localization. We refer to [17], [20] and [6] for recent localization results for divergence-form elliptic PDEs. The strategy of [17] is to construct triangulations and finite element bases that are adapted to the shape of high conductivity inclusions via coefficient dependent boundary conditions for the subgrid problems (assuming a to be piecewise constant and the number of inclusions bounded). The strategy of [20] is to solve local eigenvalue problems, observing that only a few eigenvectors are sufficient to obtain a good pre-conditioner. Both [17] and [20] require specific assumptions on the morphology and number of inclusions. The idea of the strategy is to observe that if a is piecewise constant and the number of inclusions bounded, then u is locally H^2 away from the interfaces of the inclusions. The inclusions can then be taken care of by adapting the mesh and the boundary values of localized problems or by observing that those inclusions will affect only a finite number of eigenvectors.

The strategy of [6] is to construct Generalized Finite Elements by partitioning the computational domain into to a collection of preselected subsets and compute optimal local bases (using the concept of n-widths [48]) for the approximation of harmonic functions. Local bases are constructed by solving local eigenvalue problems (corresponding to computing eigenvectors of P^*P where P is the restriction of a-harmonic functions from ω^* onto $\omega \subset \omega^*$, P^* is the adjoint of P, and ω is a sub-domain of Ω surrounded by a larger sub-domain ω^*). The method proposed in [6] achieves an exponential convergence rate (in the number of pre-computed bases functions) for harmonic functions. Non-zero right hand sides (g) are then taken care of by solving (for each different g) particular solutions on preselected subsets with a constant Neumann boundary condition (determined according to the consistency condition).

3.2 On Numerical Homogenization.

By now, the field of numerical homogenization has become large enough that it is not possible to give an exhaustive review in this short paper. Therefore, we will restrict our attention to works directly related to our work.

- The multi-scale finite element method [35, 53, 36] can be seen as a numerical generalization of this idea of oscillating test functions found in H-convergence. A convergence analysis for periodic media revealed a resonance error introduced by the microscopic boundary condition [35, 36]. An over-sampling technique was proposed to reduce the resonance error [35].

- Harmonic coordinates play an important role in various homogenization approaches, both theoretical and numerical. These coordinates were introduced in [37] in the context of random homogenization. Next, harmonic coordinates have been used in one-dimensional and quasi-one-dimensional divergence form elliptic problems [7, 5], allowing for efficient finite dimensional approximations. The connection of these coordinates with classical homogenization is made explicit in [2] in the context of multi-scale finite element methods. The idea of using particular solutions in numerical homogenization to approximate the solution space of (1.1) appears to have been first proposed in reservoir modeling in the 1980s [14], [52] (in which a global scale-up method was introduced based on generic flow solutions i.e., flows calculated from generic boundary conditions). Its rigorous mathematical analysis was done only recently [43] and is based on the fact that solutions are in fact H^2-regular with respect to harmonic coordinates (recall that they are H^1-regular with respect to Euclidean coordinates). The main message here is that if the right hand side of (1.1) is in L^2, then solutions can be approximated at small scales (in H^1-norm) by linear combinations of d (linearly independent) particular solutions (d being the dimension of the space). In that sense, harmonic coordinates are only good candidates for being d linearly independent particular solutions.

The idea of a global change of coordinates analogous to harmonic coordinates has been implemented numerically in order to up-scale porous media flows [22, 21, 14]. We refer, in particular, to a recent review article [14] for an overview of some main challenges in reservoir modeling and a description of global scale-up strategies based on generic flows.

- In [19, 24], the structure of the medium is numerically decomposed into a micro-scale and a macro-scale (meso-scale) and solutions of cell problems are computed on the micro-scale, providing local homogenized matrices that are transferred (up-scaled) to the macro-scale grid. This procedure allows one to obtain rigorous homogenization results with controlled error estimates for non-periodic media of the form $a(x, \frac{x}{\epsilon})$ (where $a(x, y)$ is assumed to be smooth in x and periodic or ergodic with specific mixing properties in y). Moreover, it is shown that the numerical algorithms associated with HMM and MsFEM can be implemented for a class of coefficients that is much broader than $a(x, \frac{x}{\epsilon})$. We refer to [29] for convergence results on the Heterogeneous Multiscale Method in the framework of G and Γ-convergence.

- More recent work includes an adaptive projection based method [42], which is consistent with homogenization when there is scale separation, leading to adaptive algorithms for solving problems with no clear scale separation; fast and sparse chaos approximations of elliptic problems with stochastic coefficients [51, 32, 18]; finite difference approximations of fully nonlinear, uniformly elliptic PDEs with Lipschitz continuous viscosity solutions [16] and operator splitting methods [4, 3].

- We refer to [12, 11] (and references therein) for most recent results on homogenization of scalar divergence-form elliptic operators with stochastic coefficients. Here, the stochastic coefficients $a(x/\varepsilon, \omega)$ are obtained from stochastic deformations (using random diffeomorphisms) of the periodic and stationary ergodic setting.

3.3 Proof of Theorem 3.1.

For each basis element φ_i of X_h, let $\psi_{i,T}$ be the solution of

$$\begin{cases} \frac{1}{T}\psi_{i,T} - \operatorname{div}(a\nabla\psi_{i,T}) = \Delta\varphi_i & \text{in} \quad \Omega \\ \psi_{i,T} = 0 & \text{on} \quad \partial\Omega \end{cases} \tag{3.8}$$

The following Proposition will allow us to control the impact of the introduction of the term $\frac{1}{T}$ in the transfer property. Observe that the domain of PDE (3.8) is still Ω (our next step will be to localize it to $\Omega_i \subset \Omega$).

Proposition 3.1. *For $g \in L^2(\Omega)$ let u be the solution of* (1.1) *in $H^1_0(\Omega)$. Then*

$$\inf_{v\in \operatorname{span}(\psi_{i,T})} \frac{\|u-v\|_{H^1_0(\Omega)}}{\|g\|_{L^2(\Omega)}} \leq C\big(h + \frac{h^2}{T}\big) \tag{3.9}$$

Proof. Let $v = \sum_i c_i\psi_{i,T}$. We have

$$\frac{u-v}{T} - \operatorname{div}\big(a\nabla(u-v)\big) = g + \frac{u}{T} - \sum_i c_i\Delta\varphi_i \tag{3.10}$$

Define $a[v]$ to be the energy norm $a[v] := \int_\Omega (\nabla v)^T a\nabla v$. Multiplying (3.10) by $u-v$ and integrating by parts, we obtain that

$$\frac{\|u-v\|^2_{L^2(\Omega)}}{T} + a[u-v] = \int_\Omega (u-v)(g + \frac{u}{T} - \sum_i c_i\Delta\varphi_i) \tag{3.11}$$

Write $c_i = c_i^1 + c_i^2$ and let w_1 and w_2 be the solutions of $\Delta w_1 = g - \sum_i c_i^1 \Delta\varphi_i$ and $\Delta w_2 = \frac{u}{T} - \sum_i c_i^2 \Delta\varphi_i$ with Dirichlet boundary conditions on $\partial\Omega$. Then, we obtain by integration by parts and the Cauchy-Schwartz inequality that

$$\frac{\|u-v\|_{L^2(\Omega)}^2}{T} + a[u-v] \leq \big\|\nabla(u-v)\big\|_{(L^2(\Omega))^d}\big(\|\nabla w_1\|_{(L^2(\Omega))^d} + \|\nabla w_2\|_{(L^2(\Omega))^d}\big) \quad (3.12)$$

Using (3.1), we can choose (c_i^1) so that

$$\|\nabla w_1\|_{(L^2(\Omega))^d} \leq Ch\|g\|_{L^2(\Omega)} \quad (3.13)$$

Using (3.2), we can choose (c_i^2) so that

$$\|\nabla w_1\|_{(L^2(\Omega))^d} \leq C\frac{h^2}{T}\|u\|_{H_0^1(\Omega)} \quad (3.14)$$

we conclude by observing that $\|u\|_{H_0^1(\Omega)} \leq C\|g\|_{L^2(\Omega)}$. □

We will now control the error induced by the localization of the elliptic problem (3.8). To this end, for each each basis element φ_i of X_h write S_i the intersection of the support of φ_i with Ω and let Ω_i be a subset of Ω containing S_i such that $\operatorname{dist}(S_i, \Omega/\Omega_i) > 0$. Let also ψ_{i,T,Ω_i} be the solution of

$$\begin{cases} \frac{1}{T}\psi_{i,T,\Omega_i} - \operatorname{div}(a\nabla\psi_{i,T,\Omega_i}) = \Delta\varphi_i & \text{in} \quad \Omega_i \\ \psi_{i,T,\Omega_i} = 0 & \text{on} \quad \partial\Omega_i \end{cases} \quad (3.15)$$

For $A, B \subset \Omega$, write $d(A,B)$ the Euclidean distance between the sets A and B.

Proposition 3.2. *Extending ψ_{i,T,Ω_i} by 0 on Ω/Ω_i we have*

$$\big\|\psi_{i,T} - \psi_{i,T,\Omega_i}\big\|_{H^1(\Omega)} \leq \frac{Ch^{\frac{d}{2}-1}(T^{-1}+1)}{\big(\operatorname{dist}(S_i,\Omega/\Omega_i)\big)^{d+1}} \exp\Big(-\frac{\operatorname{dist}(S_i,\Omega/\Omega_i)}{C\sqrt{T}}\Big) \quad (3.16)$$

We refer to Subsection 6.1 of the Appendix for the proof of Proposition 3.2.

Taking $\Omega_i := B(x_i, C_1 h^\alpha \ln\frac{1}{h}) \cap \Omega$ and $T = h^{2\alpha}$ in Proposition 3.16, we obtain for C_1 large enough (but independent from h) that

$$\big\|\psi_{i,T} - \psi_{i,T,\Omega_i}\big\|_{H^1(\Omega)} \leq Ch^{d+1} \quad (3.17)$$

Let u be the solution of (1.1) in $H_0^1(\Omega)$. Using Proposition 3.1, we obtain that there exist coefficients c_i such that

$$\big\|u - \sum_i c_i\psi_{i,T}\big\|_{H_0^1(\Omega)} \leq C\big(h + h^{2-2\alpha}\big)\|g\|_{L^2(\Omega)} \quad (3.18)$$

Using the triangle inequality, it follows that

$$\big\|u - \sum_i c_i\psi_{i,T,\Omega_i}\big\|_{H_0^1(\Omega)} \leq C\big(h + h^{2-2\alpha}\big)\|g\|_{L^2(\Omega)} + \sum_i |c_i|\big\|\psi_{i,T} - \psi_{i,T,\Omega_i}\big\|_{H^1(\Omega)} \quad (3.19)$$

whence, from Cauchy-Schwartz inequality,

$$\begin{aligned}\big\|u-\sum_i c_i\psi_{i,T,\Omega_i}\big\|_{H^1_0(\Omega)} \leq & C\big(h+h^{2-2\alpha}\big)\|g\|_{L^2(\Omega)} \\ & + \big(\sum_i |c_i|^2\big)^{\frac{1}{2}}\Big(\sum_i \big\|\psi_{i,T}-\psi_{i,T,\Omega_i}\big\|^2_{H^1(\Omega)}\Big)^{\frac{1}{2}}\end{aligned} \tag{3.20}$$

Recalling the proof of Proposition 3.1, we can choose the coefficients c_i so that

$$\|\sum_i c_i\varphi_i\|_{L^2(\Omega)} \leq \|g\|_{L^2(\Omega)} \tag{3.21}$$

Combining (3.20) with (3.4) and (3.21), we obtain that

$$\begin{aligned}\big\|u-\sum_i c_i\psi_{i,T,\Omega_i}\big\|_{H^1_0(\Omega)} \leq & C\big(h+h^{2-2\alpha}\big)\|g\|_{L^2(\Omega)} \\ & + Ch^{-\frac{d}{2}}\|g\|_{L^2(\Omega)}\Big(\sum_i \big\|\psi_{i,T}-\psi_{i,T,\Omega_i}\big\|^2_{H^1(\Omega)}\Big)^{\frac{1}{2}}\end{aligned} \tag{3.22}$$

Using (3.17) in (3.22), we obtain that

$$\big\|u-\sum_i c_i\psi_{i,T,\Omega_i}\big\|_{H^1_0(\Omega)} \leq C\big(h+h^{2-2\alpha}\big)\|g\|_{L^2(\Omega)} \tag{3.23}$$

This concludes the proof of Theorem 3.1.

3.4 On localization with high-contrast.

The constant C in the approximation error estimate (3.7) depends, a priori, on the contrast of a. Is it possible to localize the computation of bases for V_h when the contrast of a is high? The purpose of this subsection is to show that the answer is yes provided that there is a buffer zone between the boundaries of localization sub-domains and the supports of the elements φ_i where the contrast of a remains bounded. More precisely, assume that Ω is the disjoint union of $\Omega_{bounded}$ and Ω_{high}. Assume that (1.2) holds only on $\Omega_{bounded}$, and that on Ω_{high} we have

$$\lambda_{\min}(a)|\xi|^2 \leq \xi^T a(x)\xi \leq \gamma|\xi|^2. \tag{3.24}$$

where γ can be arbitrarily large. Practical examples include media characterized by a bounded contrast background with high conductivity inclusions or channels. Let ψ_i^{high} be the solution of

$$\begin{cases} h^{-2\alpha}\psi_i^{high} - \operatorname{div}(a\nabla\psi_i^{high}) = \Delta\varphi_i & \text{in} \quad \Omega_i \\ \psi_i = 0 & \text{on} \quad \partial\Omega_i \end{cases} \tag{3.25}$$

Let

$$V_h^{high} := \operatorname{span}(\psi_i^{high}) \tag{3.26}$$

be the linear space spanned by the elements ψ_i^{high}. For each i, define b_i to be the largest number r such that there exists a subset Ω_i' such that: the closure of Ω_i' contains the support of φ_i, $(\Omega_i')^r$ is a subset of Ω_i (where A^r are the set of points of Ω that are at distance at most r for A), and $(\Omega_i')^r/\Omega_i'$ is a subset of $\Omega_{bounded}$. If no such subset exists we set $b_i := 0$. b_i can be interpreted as the non-high-contrast buffer distance between the support of φ_i and the boundary of Ω_i.

Theorem 3.2. *For $g \in L^2(\Omega)$, let u be the solution of (1.1) in $H_0^1(\Omega)$ and u_h the solution of (1.1) in V_h. There exists $C_0 > 0$ such that if for all i, $b_i \geq C_0 h^\alpha \ln \frac{1}{h}$ then*

$$\frac{\|u - u_h\|_{H_0^1(\Omega)}}{\|g\|_{L^2(\Omega)}} \leq \begin{cases} Ch & \text{if} \quad \alpha \in (0, \frac{1}{2}] \\ Ch^{2-2\alpha} & \text{if} \quad \alpha \in [\frac{1}{2}, 1) \end{cases} \tag{3.27}$$

where the constants C and C_0 depend on $\lambda_{\min}(a)$, $\lambda_{\max}(a)$ (the bounds on a in $\Omega_{bounded}$), d, Ω but not on h and γ (The upper bound on a on Ω_{high}).

The proof of Theorem 3.2 is similar to that of Theorem 3.1, but it requires a precise tracking of the constants involved. The main point is to observe that the decay of the Green's function in $(\Omega_i')^r/\Omega_i'$ can be bounded independently from γ (due to the maximum principle). We will not include the proof in this paper.

4 The basis remains accurate for parabolic PDEs.

The computational gain of the method proposed in this paper is particularly significant for time-dependent problems. One such problem is the parabolic equation associated with the operator $-\operatorname{div}(a\nabla)$. More precisely, consider the time-dependent partial differential equation

$$\begin{cases} \partial_t u(x,t) - \operatorname{div}\Big(a(x)\nabla u(x,t)\Big) = g(x,t) \quad (x,t) \in \Omega_T;\ g \in L^2(\Omega_T), \\ u = 0 \quad \text{on} \quad \partial\Omega_T, \end{cases} \tag{4.1}$$

where a and Ω satisfy the same assumptions as those associated with PDE (1.1), $\Omega_T := \Omega \times [0,T]$ for some $T > 0$ and $\partial\Omega_T := (\partial\Omega \times [0,T]) \cup (\Omega \times \{t = 0\})$.

Let V_h be the finite-dimensional approximation space defined in (3.6). Let u_h be the finite element solution of (4.1), i.e. u_h can be decomposed as

$$u_h(x,t) = \sum_i c_i(t)\psi_i(x) \tag{4.2}$$

and solves for all j

$$(\psi_j, \partial_t u_h)_{L^2(\Omega)} = -a[\psi_j, u_h] + (\psi_j, g)_{L^2(\Omega)} \tag{4.3}$$

with $a[v,w] := \int_\Omega (\nabla v)^T a \nabla w$. Write

$$\|v\|^2_{L^2(0,T,H_0^1(\Omega))} := \int_0^T \int_\Omega |\nabla v|^2(x,t)\, dx\, dt \tag{4.4}$$

Theorem 4.1. *We have*

$$\big\|(u-u_h)(.,T)\big\|_{L^2(\Omega)}+\|u-u_h\|_{L^2(0,T,H^1_0(\Omega))}\leq C\|g\|_{L^2(\Omega_T)}(h+h^{2-2\alpha}) \tag{4.5}$$

Proof. The proof is a generalization of the proof found in [44] (in which approximation spaces are constructed via harmonic coordinates). Let $\mathcal{A}_T$ be the bilinear form on $L^2(0,T,H^1_0(\Omega))$ defined by

$$\mathcal{A}_T[w_1,w_2]:=\int_0^T a[w_1,w_2]\,dt \tag{4.6}$$

Observe that for all $v\in L^2(0,T,V_h)$,

$$\big(v,\partial_t(u-u_h)\big)_{L^2(\Omega_T)}+\mathcal{A}_T[v,u-u_h]=0 \tag{4.7}$$

Writing $\mathcal{A}_T[v]:=\mathcal{A}_T[v,v]$, we deduce that for $v\in L^2(0,T,V_h)$,

$$\begin{gathered}\frac{1}{2}\big\|(u-u_h)(.,T)\big\|^2_{L^2(\Omega)}+\mathcal{A}_T[u-u_h]=\\ \big(u-v,\partial_t(u-u_h)\big)_{L^2(\Omega_T)}+\mathcal{A}_T[u-v,u-u_h]\end{gathered} \tag{4.8}$$

Using $\partial_t u_h$ in (4.3) and integrating, we obtain that

$$\|\partial_t u_h\|^2_{L^2(\Omega_T)}+\frac{1}{2}a\big[u_h(.,T),u_h(.,T)\big]=\big(\partial_t u_h,g\big)_{L^2(\Omega_T)} \tag{4.9}$$

Using Minkowski's inequality, we deduce that

$$\|\partial_t u_h\|^2_{L^2(\Omega_T)}+a\big[u_h(.,T),u_h(.,T)\big]\leq C\|g\|^2_{L^2(\Omega_T)} \tag{4.10}$$

Similarly,

$$\|\partial_t u\|^2_{L^2(\Omega_T)}+a\big[u(.,T),u(.,T)\big]\leq C\|g\|^2_{L^2(\Omega_T)} \tag{4.11}$$

Using Cauchy-Schwartz and Minkowski inequalities in (4.8), we obtain that

$$\big\|(u-u_h)(.,T)\big\|^2_{L^2(\Omega)}+\mathcal{A}_T[u-u_h]\leq C\|u-v\|_{L^2(\Omega_T)}\|g\|_{L^2(\Omega_T)}+C\mathcal{A}_T[u-v] \tag{4.12}$$

Take $v=\mathcal{R}_h u$ to be the projection of u onto $L^2(0,T,V_h)$ with respect to the bilinear form $\mathcal{A}_T$. Observing that $-\operatorname{div}(a\nabla u)=g-\partial_t u$ with $(g-\partial_t u)\in L^2(\Omega_T)$, we obtain from Theorem 3.1 that

$$\big(\mathcal{A}_T[u-\mathcal{R}_h u]\big)^{\frac{1}{2}}\leq C\|g\|_{L^2(\Omega_T)}(h+h^{2-2\alpha}) \tag{4.13}$$

Let us now show (using a standard duality argument) that

$$\|u-\mathcal{R}_h u\|_{L^2(\Omega_T)}\leq C(h+h^{2-2\alpha})^2\|g\|_{L^2(\Omega_T)} \tag{4.14}$$

Choose v^* to be the solution of the following linear problem: For all $w\in L^2(0,T,H^1_0(\Omega))$

$$\mathcal{A}_T[w,v^*]=(w,u-\mathcal{R}_h u)_{L^2(\Omega_T)} \tag{4.15}$$

Taking $w = u - \mathcal{R}_h u$ in (4.15), we obtain that

$$\|u - \mathcal{R}_h u\|^2_{L^2(\Omega_T)} = \mathcal{A}_T[u - \mathcal{R}_h u, v^* - \mathcal{R}_h v^*] \tag{4.16}$$

Hence by Cauchy Schwartz inequality and (4.13),

$$\|u - \mathcal{R}_h u\|^2_{L^2(\Omega_T)} \leq C(h + h^{2-2\alpha})\|g\|_{L^2(\Omega_T)}\big(\mathcal{A}_T[v^* - \mathcal{R}_h v^*]\big)^{\frac{1}{2}} \tag{4.17}$$

Using Theorem 3.1 again, we obtain that

$$\big(\mathcal{A}_T[v^* - \mathcal{R}_h v^*]\big)^{\frac{1}{2}} \leq C\|u - \mathcal{R}_h u\|_{L^2(\Omega_T)}(h + h^{2-2\alpha}) \tag{4.18}$$

Combining (4.18) with (4.17) leads to (4.14). Combining (4.12) with $v = \mathcal{R}_h u$, (4.14) and (4.13) leads to

$$\big\|(u - u_h)(.,T)\big\|^2_{L^2(\Omega)} + \mathcal{A}_T[u - u_h] \leq C(h + h^{2-2\alpha})^2\|g\|^2_{L^2(\Omega_T)} \tag{4.19}$$

which concludes the proof of Theorem 4.1. □

Discretization in time. Let (t_n) be a discretization of $[0,T]$ with time-steps $|t_{n+1} - t_n| = \Delta t$. Write Z^h_T, the subspace of $L^2(0,T,V_h)$, such that

$$Z^h_T = \left\{ v \in L^2(0,T,V_h) \,:\, v(x,t) = \sum_i c_i(t)\psi_i(x),\ c_i(t) \text{ are constants on } (t_n, t_{n+1}] \right\}. \tag{4.20}$$

Write $u_{h,\Delta t}$, the solution in Z^h_T of the following system of implicit weak formulation (such that $u_{h,\Delta t}(x,0) \equiv 0$): For each n and $\psi \in V_h$,

$$\begin{aligned} \big(\psi, u_{h,\Delta t}(t_{n+1})\big)_{L^2(\Omega)} =& \big(\psi, u_{h,\Delta t}(t_n)\big)_{L^2(\Omega)} \\ & - |\Delta t|\, a\big[\psi, u_{h,\Delta t}(t_{n+1})] + \big(\psi, \int_{t_n}^{t_{n+1}} g(t)\, dt\big)_{L^2(\Omega)}. \end{aligned} \tag{4.21}$$

Then, we have the following theorem

Theorem 4.2. *We have*

$$\begin{aligned} \big\|(u - u_{h,\Delta t})(T)\big\|_{L^2(\Omega)} + \|u - u_{h,\Delta t}\|_{L^2(0,T,H^1_0(\Omega))} \leq& C\big(|\Delta t| + h + h^{2-2\alpha}\big) \\ & \Big(\|\partial_t g\|_{L^2(0,T,H^{-1}(\Omega))} + \big\|g(.,0)\big\|_{L^2(\Omega)} + \|g\|_{L^2(\Omega_T)}\Big). \end{aligned} \tag{4.22}$$

The proof of Theorem 4.2 is similar to that of Theorem 1.6 of [44] and will not be given here. Observe that homogenization in space allows for a discretization in time with time steps $\mathcal{O}(h + h^{2-2\alpha})$ without compromising the accuracy of the method.

5 The basis remains accurate for hyperbolic PDEs.

Consider the hyperbolic partial differential equation

$$\begin{cases} \rho(x)\partial_t^2 u(x,t) - \operatorname{div}\Big(a(x)\nabla u(x,t)\Big) = g(x,t) \quad (x,t) \in \Omega_T;\, g \in L^2(\Omega_T), \\ u = 0 \quad \text{on} \quad \partial\Omega_T, \\ \partial_t u = 0 \quad \text{on} \quad \Omega \times t = 0 \end{cases} \tag{5.1}$$

Where a, Ω, Ω_T and $\partial\Omega_T$ are defined as in Section 4. In particular, a is assumed to be only uniformly elliptic and bounded ($a_{i,j} \in L^\infty(\Omega)$). We will further assume that ρ is uniformly bounded from below and above ($\rho \in L^\infty(\Omega)$ and $\operatorname{essinf} \rho(x) \geq \rho_{\min} > 0$). It is straightforward to extend the results presented here to nonzero boundary conditions (provided that frequencies larger than $1/h$ remain weakly excited, because the waves equation preserves energy and homogenization schemes can not recover energies put into high frequencies, see [45]). For the sake of conciseness, we will give those results with zero boundary conditions. PDE (5.1) corresponds to acoustic wave equations in a medium with density ρ and bulk modulus a^{-1}.

Let V_h be the finite-dimensional approximation space defined in (3.6). Let u_h be the finite element solution of (5.1), i.e. u_h can be decomposed as

$$u_h(x,t) = \sum_i c_i(t)\psi_i(x) \tag{5.2}$$

and solves for all j

$$(\psi_j, \partial_t^2 u_h)_{L^2(\rho,\Omega)} = -a[\psi_j, u_h] + (\psi_j, g)_{L^2(\Omega)} \tag{5.3}$$

where

$$(v,w)_{L^2(\rho,\Omega)} := \int_\Omega v\, w\, \rho \tag{5.4}$$

Theorem 5.1. *If $\partial_t g \in L^2(\Omega_T)$ and $g(x,0) \in L^2(\Omega)$, then*

$$\begin{aligned} \big\|\partial_t(u-u_h)(.,T)\big\|_{L^2(\Omega)} + \big\|(u-u_h)(.,T)\big\|_{L^2(H_0^1(\Omega))} \leq \\ C\big(\|\partial_t g\|_{L^2(\Omega_T)} + \|g(x,0)\|_{L^2(\Omega)}\big)(h + h^{2-2\alpha}) \end{aligned} \tag{5.5}$$

Remark 5.1. We refer to [45] for an alternative strategy based on harmonic coordinates. We refer to [23] and [1] for HMM based methods. Homogenization based methods require that frequencies larger than $1/h$ remain weakly excited. For high frequencies, and away from local resonances (e.g. local, nearly resonant, cavities), we refer to the sweeping pre-conditioner method [25, 26].

Proof. Let $\mathcal{A}_T$ be the bilinear form on $L^2(0,T,H_0^1(\Omega))$ defined in (4.6). Observe that for all $v \in L^2(0,T,V_h)$,

$$\big(v, \partial_t^2(u-u_h)\big)_{L^2(\rho,\Omega_T)} + \mathcal{A}_T[v, u-u_h] = 0 \tag{5.6}$$

Taking $\partial_t u - \partial_t u_h - (\partial_t u - \partial_t v)$ as a test function in (5.6) and integrating in time, we deduce that for $\partial_t v \in L^2(0,T,V_h)$,

$$\begin{aligned} &\frac{1}{2}\big\|\partial_t(u-u_h)(.,T)\big\|^2_{L^2(\rho,\Omega)} + \frac{1}{2}a\big[(u-u_h)(.,T)\big] = \\ &\quad \big(\partial_t(u-v), \partial_t^2(u-u_h)\big)_{L^2(\rho,\Omega_T)} + \mathcal{A}_T[\partial_t(u-v), u-u_h] \end{aligned} \tag{5.7}$$

where $(v,w)_{L^2(\rho,\Omega_T)} := \int_0^T \int_\Omega v\, w\, \rho\, dx\, dt$. Taking the derivative of the hyperbolic equation for u in time, we obtain that

$$\partial_t^3 u - \operatorname{div}(a\nabla\partial_t u) = \partial_t g \tag{5.8}$$

Integrating (5.8) against the test function $\partial_t^2 u$ and observing that $\partial_t^2 u(x,0) = g(x,0)$, we also obtain that

$$\big\|\partial_t^2 u(.,T)\big\|^2_{L^2(\rho,\Omega)} + a\big[\partial_t u(.,T)\big] \leq C\big(\|\partial_t g\|^2_{L^2(\Omega_T)} + \|g(x,0)\|^2_{L^2(\Omega)}\big) \tag{5.9}$$

Similarly, we obtain that

$$\big\|\partial_t^2 u_h(.,T)\big\|^2_{L^2(\rho,\Omega)} + a\big[\partial_t u_h(.,T)\big] \leq C\big(\|\partial_t g\|^2_{L^2(\Omega_T)} + \|g(x,0)\|^2_{L^2(\Omega)}\big) \tag{5.10}$$

Take $\partial_t v = \mathcal{R}_h \partial_t u$ to be the projection of $\partial_t u$ onto $L^2(0,T,V_h)$ with respect to the bilinear form $\mathcal{A}_T$. Observing that $-\operatorname{div}(a\nabla\partial_t u) = \partial_t g - \partial_t^2 u$ with $(g - \partial_t^2 u) \in L^2(\Omega_T)$, we obtain from (5.9) and Theorem 3.1 that

$$\big(\mathcal{A}_T[u - \mathcal{R}_h u]\big)^{\frac{1}{2}} \leq C\big(\|\partial_t g\|_{L^2(\Omega_T)} + \|g(x,0)\|_{L^2(\Omega)}\big)(h + h^{2-2\alpha}) \tag{5.11}$$

Furthermore, using the same duality argument as in the parabolic case, we obtain that

$$\|u - \mathcal{R}_h u\|_{L^2(\rho,\Omega_T)} \leq C(h + h^{2-2\alpha})^2\big(\|\partial_t g\|_{L^2(\Omega_T)} + \|g(x,0)\|_{L^2(\Omega)}\big) \tag{5.12}$$

Using Cauchy-Schwartz and Minkowski inequalities and the above estimates in (5.7), we obtain that

$$\begin{aligned} &\big\|\partial_t(u-u_h)(.,T)\big\|^2_{L^2(\rho,\Omega)} + a\big[(u-u_h)(.,T)\big] \leq \\ &C(h + h^{2-2\alpha})\big(\mathcal{A}_T[u-u_h] + \|\partial_t g\|_{L^2(\Omega_T)} + \|g(x,0)\|_{L^2(\Omega)}\big) \end{aligned} \tag{5.13}$$

We conclude using Grownwall's lemma. □

6 Appendix

6.1 Proof of Proposition 3.2.

The proof of Proposition 3.2 is a generalization of the proof of the control of the resonance error in periodic medium given in [30].

First we need the following lemma, which is the cornerstone of Cacciopoli's inequality.

Lemma 6.1. *Let D be a sub-domain of Ω with piecewise Lipschitz boundary, and let v solve*

$$\begin{cases} \frac{v}{T} - \operatorname{div}\Big(a(x)\nabla v(x)\Big) = f(x) \quad x \in D; f \in H^{-1}(D), \\ v = 0 \quad on \quad \partial D, \end{cases} \tag{6.1}$$

Let $\zeta : D \to \mathbb{R}^+$ be a function of class C^1 such that ζ is identically null on an open neighborhood of the support of f. Then,

$$\int_D \big|\nabla(\zeta v)\big|^2 \leq C \int_D v^2 |\nabla \zeta|^2 \tag{6.2}$$

where C only depends on the essential supremum and infimum of the maximum and minimum eigenvalues of a over D.

Proof. Multiplying (6.1) by $\zeta^2 v$ and integrating by parts, we obtain that

$$\int_D \zeta \frac{v^2}{T} + \int_D \nabla(\zeta^2 v) a \nabla v = 0 \tag{6.3}$$

Hence,

$$\int_D \zeta \frac{v^2}{T} + \int_D \nabla(\zeta v) a \nabla(\zeta v) = \int_D v^2 \nabla \zeta a \nabla \zeta \tag{6.4}$$

Which concludes the proof. □

Lemma 6.2. *Let D be a sub-domain of Ω with piecewise Lipschitz boundary. Write $G_{T,D}$ the Green's function of the operator $\frac{1}{T} - \operatorname{div}(a\nabla)$ with Dirichlet boundary condition on ∂D. Then,*

$$G_{T,D}(x,y) \leq \frac{C}{|x-y|^{d-2}} \exp\big(-\frac{|x-y|}{C\sqrt{T}}\big) \tag{6.5}$$

where C only depends on d and the essential supremum and infimum of the maximum and minimum eigenvalues of a over D.

Proof. Extending a to $\mathbb{R}^d$ and using the maximum principle, we obtain that

$$G_{T,D}(x,y) \leq G_{T,\mathbb{R}^d}(x,y) \tag{6.6}$$

we conclude by using the exponential decay of the Green's function in $\mathbb{R}^d$ (we refer to Lemma 2 of [30]). □

Lemma 6.3. *Let $\psi_{i,T}$ be the solution of (3.8) and ψ_{i,T,Ω_i} the solution of (3.15). Let Ω_i' be a sub-domain of Ω_i such that $S_i \subset \Omega_i'$ and $\operatorname{dist}(S_i, \Omega_i/\Omega_i') > 0$. We have*

$$\big\|\psi_{i,T}\big\|_{H^1(\Omega/\Omega_i')} \leq \frac{Ch^{\frac{d}{2}-1}}{\big(\operatorname{dist}(S_i,\Omega/\Omega_i')\big)^d} \exp\Big(-\frac{\operatorname{dist}(S_i,\Omega/\Omega_i')}{C\sqrt{T}}\Big) \tag{6.7}$$

and

$$\big\|\psi_{i,T,\Omega_i}\big\|_{H^1(\Omega_i/\Omega_i')} \leq \frac{Ch^{\frac{d}{2}-1}}{\big(\operatorname{dist}(S_i,\Omega/\Omega_i')\big)^d} \exp\Big(-\frac{\operatorname{dist}(S_i,\Omega/\Omega_i')}{C\sqrt{T}}\Big) \tag{6.8}$$

Proof. For $A \subset \Omega$, write A^r the set of points of Ω that are at distance at most r from A. Let us now use Cacciopoli's inequality to bound $\int_{\Omega/\Omega_i'} |\nabla\psi_{i,T}|^2$. Using Lemma 6.1 with ζ identically equal to one on Ω/Ω_i', zero on $(\Omega/\Omega_i')^r$ with $r := \operatorname{dist}(S_i, \Omega/\Omega_i')/3$ and $|\nabla\zeta| \leq C/r$, we obtain that

$$\int_{\Omega/\Omega_i'} |\nabla\psi_{i,T}|^2 \leq \frac{C}{r^2} \int_{(\Omega/\Omega_i')^r} \psi_{i,T}^2 \tag{6.9}$$

Next, observe that for $x \in (\Omega/\Omega_i')^r$,

$$\psi_{i,T}(x) = -\int_{S_i} \nabla G_{T,\Omega}(x,y) \nabla\varphi_i(y)\, dy \tag{6.10}$$

Hence,

$$\big|\psi_{i,T}(x)\big| \leq \|\nabla\varphi_i\|_{(L^2(S_i))^d} \big\|\nabla G_{T,\Omega}(x,.)\big\|_{(L^2(S_i))^d} \tag{6.11}$$

Another use of Cacciopoli's inequality leads to

$$\big\|\nabla G_{T,\Omega}(x,.)\big\|_{(L^2(S_i))^d} \leq \frac{C}{r} \big\|G_{T,\Omega}(x,.)\big\|_{L^2(S_i^r)} \tag{6.12}$$

Combining (6.9) with (6.11) with (6.12), we obtain that

$$\int_{\Omega/\Omega_i'} |\nabla\psi_{i,T}|^2 \leq \|\nabla\varphi_i\|^2_{(L^2(S_i))^d} \frac{C}{r^4} \int_{(\Omega/\Omega_i')^r} \big\|G_{T,\Omega}(x,.)\big\|^2_{L^2(S_i^r)} \tag{6.13}$$

We conclude the proof of (6.7) using Lemma 6.2 and (3.3). The proof of (6.8) is similar observing that $\operatorname{dist}(S_i, \Omega/\Omega_i') \leq \operatorname{dist}(S_i, \Omega_i/\Omega_i')$ ∎

Lemma 6.4. *Let D be a sub-domain of Ω with piecewise Lipschitz boundary. Let $\psi \in H^1(\Omega)$, and let v solve*

$$\begin{cases} \frac{v}{T} - \operatorname{div}\Big(a(x)\nabla v(x)\Big) = 0 \quad x \in D, \\ v = \psi \quad \text{on} \quad \partial D, \end{cases} \tag{6.14}$$

Write S the intersection of the support of ψ with D. Let D_1 be a sub-domain of D such that $\operatorname{dist}(D_1, S) > 0$, then

$$\int_{D_1} |\nabla v|^2 \leq \frac{C}{\big(\operatorname{dist}(D_1,S)\big)^{2d}} (T^{-1}+1)^2 \|\psi\|^2_{H^1(\Omega)} \exp\Big(-\frac{\operatorname{dist}(D_1,S)}{C\sqrt{T}}\Big) \tag{6.15}$$

where C does not depend on D, D_1, S.

Proof. Write $w := v - \psi$. Then,

$$\begin{cases} \frac{w}{T} - \operatorname{div}\Big(a(x)\nabla w(x)\Big) = -\frac{\psi}{T} + \operatorname{div}(a\nabla\psi) \quad x \in D, \\ v = 0 \quad \text{on} \quad \partial D, \end{cases} \tag{6.16}$$

Thus,

$$w(x) = -\int_D \big(\frac{\psi(y)}{T} G_{T,D}(x,y) + \nabla\psi(y) a(y) \nabla G_{T,D}(x,y)\big)\, dy \tag{6.17}$$

Using Cauchy-Schwartz inequality, we obtain that

$$|w(x)| \leq C\|\psi\|_{H^1(\Omega)} \Big(\frac{1}{T}\big\|G_{T,D}(x,.)\big\|_{L^2(S)} + \big\|\nabla G_{T,D}(x,.)\big\|_{(L^2(S))^d}\Big) \tag{6.18}$$

For $A \subset D$, write A^r the set of points of D that are at distance at most r from A. Let us now use Cacciopoli's inequality to bound $\int_{D_1} |\nabla w|^2$. Using Lemma 6.1 with ζ identically equal to one on D_1, zero on $D/D_1^{r_1}$ and such that $|\nabla\zeta| \leq C/r_1$ we obtain that

$$\int_{D_1} |\nabla w|^2 \leq \frac{C}{r_1^2} \int_{D_1^{r_1}} w^2 \tag{6.19}$$

provided that $\operatorname{dist}(D_1^{r_1}, S) > 0$. Hence, for $r_1 := \operatorname{dist}(D_1, S)/3$, we obtain (6.19). Taking $r_2 := \operatorname{dist}(D_1, S)/3$ and using Cacciopoli's inequality again, we also obtain that

$$\big\|\nabla G_{T,D}(x,.)\big\|_{(L^2(S))^d} \leq \frac{C}{r_2}\big\|G_{T,D}(x,.)\big\|_{L^2(S^{r_2})} \tag{6.20}$$

Combining (6.19) with (6.18) and (6.20) and observing that $w = v$ on $D_1^{r_1}$ we obtain that

$$\int_{D_1} |\nabla v|^2 \leq \frac{C}{r_1^2 r_2^2} \|\psi\|^2_{H^1(\Omega)} (T^{-1}+1)^2 \int_{D_1^{r_1}} \big\|G_{T,D}(x,.)\big\|^2_{L^2(S^{r_2})} \tag{6.21}$$

Using Lemma 6.2, we deduce that

$$\int_{D_1} |\nabla w|^2 \leq \frac{C|\Omega|}{(\operatorname{dist}(D_1,S))^{2d}} \|\psi\|^2_{H^1(\Omega)} (T^{-1}+1)^2 \exp\big(-\frac{\operatorname{dist}(D_1,S)}{C\sqrt{T}}\big) \tag{6.22}$$

This concludes the proof of Lemma 6.4. □

Lemma 6.5. *Let $\psi_{i,T}$ be the solution of* (3.8) *and ψ_{i,T,Ω_i} the solution of* (3.15)*. Let Ω_i' be a sub-domain of Ω_i such that* $\operatorname{dist}(\Omega/\Omega_i, \Omega_i') > 0$*. We have*

$$\big\|\psi_{i,T} - \psi_{i,T,\Omega_i}\big\|_{H^1(\Omega_i')} \leq \frac{C(T^{-1}+1)h^{\frac{d}{2}-1}}{\big(\operatorname{dist}(\Omega/\Omega_i,\Omega_i')\big)^{d+1}} \exp\Big(-\frac{\operatorname{dist}(\Omega/\Omega_i,\Omega_i')}{C\sqrt{T}}\Big) \tag{6.23}$$

Proof. Lemma 6.5 is a direct consequence of Lemma 6.4. To this end, we choose $D := \Omega_i$, $v =: \psi_{i,T} - \psi_{i,T,\Omega_i}$ and $D_1 := \Omega_i'$. We also choose $\psi := \eta\psi_{i,T}$ where $\eta : \Omega \to [0,1]$ is C^1, equal to one on Ω/Ω_i and 0 on $(\Omega/\Omega_i)^r$ with $r := \operatorname{dist}(\Omega/\Omega_i, \Omega_i')/3$ (A^r being the set of points in Ω at distance at most r from A) and $|\nabla\eta| \leq C/r$. We obtain from Lemma 6.4 that

$$\big\|\psi_{i,T} - \psi_{i,T,\Omega_i}\big\|_{H^1(\Omega_i')} \leq \frac{C(T^{-1}+1)}{\big(\operatorname{dist}(\Omega/\Omega_i,\Omega_i')\big)^{d}} \|\psi\|_{H^1(\Omega)} \exp\Big(-\frac{\operatorname{dist}(\Omega/\Omega_i,\Omega_i')}{C\sqrt{T}}\Big) \tag{6.24}$$

We conclude using (3.3) and $\|\psi\|_{H^1(\Omega)} \leq \frac{C}{\operatorname{dist}(\Omega/\Omega_i,\Omega_i')}\|\nabla\varphi_i\|_{(L^2(\Omega))^d}$. □

h	L^2	H^1	L^∞
0.5	0.0119	0.0913	0.0157
0.25	0.0057	0.0664	0.0115
0.125	0.0027	0.0482	0.0075
0.0625	0.0005	0.0207	0.0032

Table 1: Example 1 of Section 3 of [43] (trigonometric multi-scale, see also [39]) with $\alpha = 1/2$.

Observing that

$$\left\|\psi_{i,T} - \psi_{i,T,\Omega_i}\right\|_{H^1(\Omega)} \leq \left\|\psi_{i,T} - \psi_{i,T,\Omega_i}\right\|_{H^1(\Omega_i')} + \left\|\psi_{i,T}\right\|_{H^1(\Omega/\Omega_i')} + \left\|\psi_{i,T,\Omega_i}\right\|_{H^1(\Omega_i/\Omega_i')}, \tag{6.25}$$

we conclude the proof of Proposition 3.2 by using Lemma 6.5 and Lemma 6.3 with $\Omega_i' := S_i^r$ where S_i^r are the points in Ω_i at distance at most r from S_i with $r := \mathrm{dist}(S_i, \Omega/\Omega_i)/3$.

6.2 Numerical experiments.

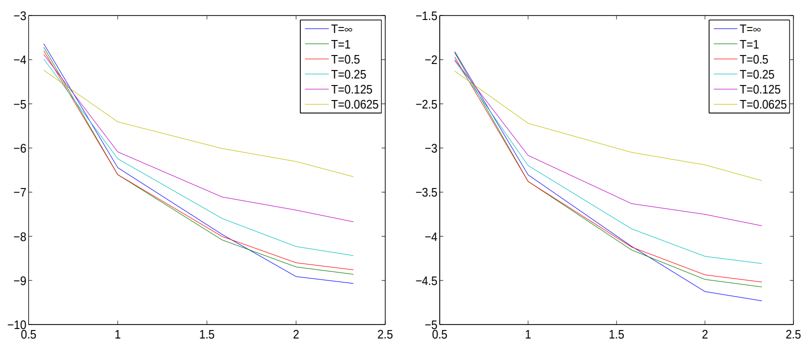

(a) L^2 ***error*** **(b)** H^1 ***error***

Figure 1: Example 5 of Section 3 of [43] (percolation at criticality). Logarithm (in base 2) of the error with respect to $\log_2(h_0/h)$ (for $h = 0.125$) and the value of T used in (3.5).

Elliptic equation. We compute the solutions of (1.1) up to time 1 on the fine mesh and in the finite-dimensional approximation space V_h defined in (3.6). The physical domain is the square $[-1,1]^2$. Global equations are solved on a fine triangulation with 66049 nodes and 131072 triangles.

The elements (φ_i) of Sub-section 3.1 are weighted extended B-splines (WEB) [33, 34] (obtained by tensorizing one-dimensional elements and using weight function $(1-x^2)(1-$

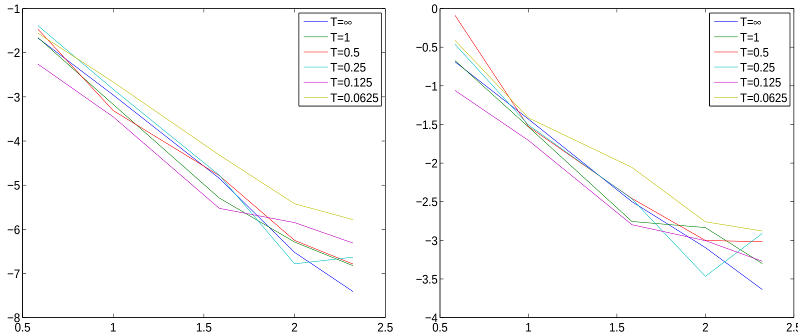

(a) L^2 ***error*** **(b)** H^1 ***error***

Figure 2: Example 3 of Section 3 of [43] (exponential of a sum of trigonometric functions with strongly overlapping frequencies). Logarithm (in base 2) of the error with respect to $\log_2(h_0/h)$ (for $h = 0.125$) and the value of T used in (3.5).

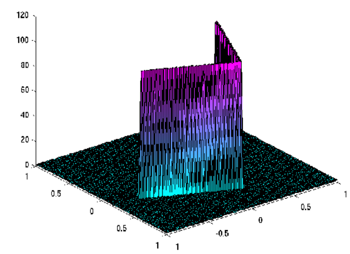

Figure 3: High conductivity channel.

y^2) to enforce the Dirichlet boundary condition). We write h the size of the coarse mesh. Elements ψ_i are obtained by solving (3.5) on localized sub-domains of size h_0. Table 1 shows errors with $\alpha = 1/2$ for a given by (6.26) (Example 1 of Section 3 of [43], trigonometric multi-scale, see also [39]), i.e. for

$$\begin{aligned} a(x) := &\frac{1}{6}\Big(\frac{1.1+\sin(2\pi x/\epsilon_1)}{1.1+\sin(2\pi y/\epsilon_1)} + \frac{1.1+\sin(2\pi y/\epsilon_2)}{1.1+\cos(2\pi x/\epsilon_2)} + \frac{1.1+\cos(2\pi x/\epsilon_3)}{1.1+\sin(2\pi y/\epsilon_3)} + \\ &\frac{1.1+\sin(2\pi y/\epsilon_4)}{1.1+\cos(2\pi x/\epsilon_4)} + \frac{1.1+\cos(2\pi x/\epsilon_5)}{1.1+\sin(2\pi y/\epsilon_5)} + \sin(4x^2y^2) + 1\Big) \end{aligned} \tag{6.26}$$

where $\epsilon_1 = \frac{1}{5}$,$\epsilon_2 = \frac{1}{13}$,$\epsilon_3 = \frac{1}{17}$,$\epsilon_4 = \frac{1}{31}$,$\epsilon_5 = \frac{1}{65}$.

Figure 1 shows the logarithm (in base 2) of the error with respect to $\log_2(h_0/h)$ (for $h = 0.125$) and the value of T used in (3.5) for a given by Example 5 of Section 3 of [43] (percolation at criticality, the conductivity of each site is equal to γ or $1/\gamma$ with

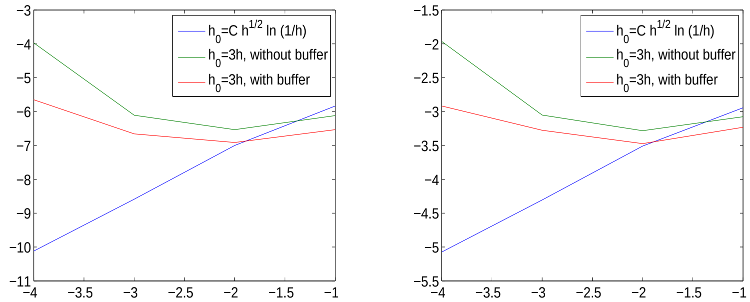

(a) L^2 ***error*** **(b)** H^1 ***error***

Figure 4: High conductivity channel (Figure 3). The x-axis shows $\log_2(h)$, the y-axis shows the $\log_2$ of the error in L^2 and H^1-norm. The three cases for the localization are $h_0 = \mathcal{O}(\sqrt{h}\ln\frac{1}{h})$ with a buffer around the high conductivity channel (see Sub-section 3.4) of size $\mathcal{O}(\sqrt{h}\ln\frac{1}{h})$, $h_0 = 3h$ with no buffer around the high conductivity channel and $h_0 = 3h$ with a buffer around the high conductivity channel of size $3h$.

probability 1/2 and $\gamma = 4$).

Figure 2 shows the logarithm (in base 2) of the error with respect to $\log_2(h_0/h)$ (for $h = 0.125$) and the value of T used in (3.5) for a given by Example 3 of Section 3 of [43], i.e. $a(x) = e^{h(x)}$, with $h(x) = \sum_{|k|\leq R}(a_k \sin(2\pi k \cdot x) + b_k \cos(2\pi k \cdot x))$, where a_k and b_k are independent uniformly distributed random variables on $[-0.3, 0.3]$ and $R = 6$.

High contrast, with and without buffer. In this example, a is characterized by a fine and long-ranged high conductivity channel (Figure 3). We choose $a(x) = 100$, if x is in the channel, and $a(x)$ is the percolation medium, if x is not in the channel (the conductivity of each site, not in channel, is equal to γ or $1/\gamma$ with probability 1/2 and $\gamma = 4$). Figure 4 shows the log_2 of the numerical error (in L^2 and H^1 norm) versus $log_2(h)$. The three cases for the localization are $h_0 = \mathcal{O}(\sqrt{h}\ln\frac{1}{h})$ with a buffer around the high conductivity channel (see Sub-section 3.4) of size $\mathcal{O}(\sqrt{h}\ln\frac{1}{h})$, $h_0 = 3h$ with no buffer around the high conductivity channel and $h_0 = 3h$ with a buffer around the high conductivity channel of size $3h$. The first case shows that the method of Sub-section 3.4 is converging as expected. The second case shows that, as expected, taking $\alpha = 1$, does not guarantee convergence. The third case shows that adding a buffer around the high conductivity channel improves numerical errors but is not sufficient to guarantee convergence (as expected, we also need $\alpha < 1$). The percolating background medium has been re-sampled for each case; the effect of this re-sampling can be seen for the largest value of h (i.e. $\log_2(h) = -1$).

Wave equation. We compute the solutions of (5.1) up to time 1 on the fine mesh and in the finite-dimensional approximation space V_h defined in (3.6). The initial condition

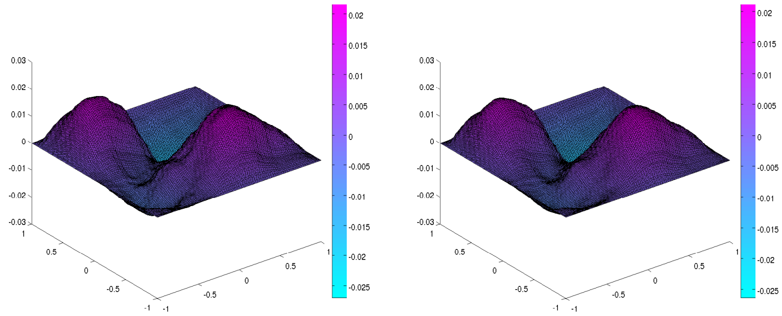

(a) u **(b)** u_h

Figure 5: Wave equation. Trigonometric case, fine mesh solution, $h = 0.125$, $h_0 = 3h$, $T = h$. The L^2, H^1 and L^∞ relative numerical errors are 0.0339, 0.1760 and 0.0235.

is $u(x, 0) = 0$ and $u_t(x, 0) = 0$. The boundary condition is $u(x, t) = 0$, for $x \in \partial\Omega$. The density is uniformly equal to one and we choose $g = \sin(\pi x)\sin(\pi y)$. Figure 5 shows the fine mesh solutions u and u_h at time one, for a given by the trigonometric example (6.26), with $h = 0.125$, $h_0 = 3h$ and $T = h$. Figure 5 shows the fine mesh solutions u and u_h at time one, for a given by the high conductivity channel example (Figure 3), with $h = 0.125$, $h_0 = 3h$ and $T = h$.

Acknowledgements. We thank L. Berlyand for stimulating discussions. We also thank Ivo Babuška, John Osborn, George Papanicolaou and Björn Engquist for pointing us in the direction of the localization problem. The work of H. Owhadi is partially supported by the National Science Foundation under Award Number CMMI-092600 and the Department of Energy National Nuclear Security Administration under Award Number DE-FC52-08NA28613. We thank Sydney Garstang for proofreading the manuscript.

References

[1] A. Abdulle and M.J. Grote. Finite element heterogeneous multiscale method for the wave equation. *Submitted*, 2010.

[2] G. Allaire and R. Brizzi. A multiscale finite element method for numerical homogenization. *Multiscale Model. Simul.*, 4(3):790–812 (electronic), 2005.

[3] T. Arbogast and K. J. Boyd. Subgrid upscaling and mixed multiscale finite elements. *SIAM J. Numer. Anal.*, 44(3):1150–1171 (electronic), 2006.

[4] T. Arbogast, C.-S. Huang, and S.-M. Yang. Improved accuracy for alternating-direction methods for parabolic equations based on regular and mixed finite elements. *Math. Models Methods Appl. Sci.*, 17(8):1279–1305, 2007.

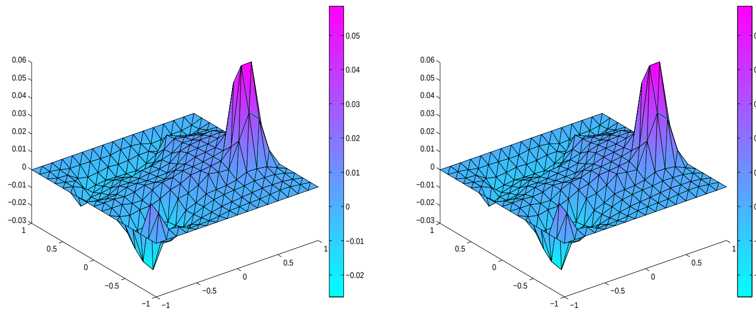

(a) u **(b)** u_h

Figure 6: Wave equation. Channel case, coarse mesh solution, $h = 0.125$, $h_0 = 3h$, $T = h$. The L^2, H^1 and L^∞ relative numerical errors are 0.0439, 0.2684 and 0.0389.

[5] I. Babuška, G. Caloz, and J. E. Osborn. Special finite element methods for a class of second order elliptic problems with rough coefficients. *SIAM J. Numer. Anal.*, 31(4):945–981, 1994.

[6] I. Babuška and R. Lipton. Optimal local approximation spaces for generalized finite element methods with application to multiscale problems. *arXiv:1004.3041*, 2010.

[7] I. Babuška and J. E. Osborn. Generalized finite element methods: their performance and their relation to mixed methods. *SIAM J. Numer. Anal.*, 20(3):510–536, 1983.

[8] A. Bensoussan, J. L. Lions, and G. Papanicolaou. *Asymptotic analysis for periodic structure*. North Holland, Amsterdam, 1978.

[9] L. Berlyand and H. Owhadi. Flux norm approach to finite dimensional homogenization approximations with non-separated scales and high contrast. *Archives for Rational Mechanics and Analysis*, 198(2):677–721, 2010.

[10] C. Bernardi and R. Verfürth. Adaptive finite element methods for elliptic equations with non-smooth coefficients. *Numer. Math.*, 85(4):579–608, 2000.

[11] X. Blanc, C. Le Bris, and P.-L. Lions. Une variante de la théorie de l'homogénéisation stochastique des opérateurs elliptiques. *C. R. Math. Acad. Sci. Paris*, 343(11-12):717–724, 2006.

[12] X. Blanc, C. Le Bris, and P.-L. Lions. Stochastic homogenization and random lattices. *J. Math. Pures Appl. (9)*, 88(1):34–63, 2007.

[13] A. Braides. *Γ-convergence for beginners*, volume 22 of *Oxford Lecture Series in Mathematics and its Applications*. Oxford University Press, Oxford, 2002.

[14] L. V. Branets, S. S. Ghai, L. L., and X.-H. Wu. Challenges and technologies in reservoir modeling. *Commun. Comput. Phys.*, 6(1):1–23, 2009.

[15] S. C. Brenner and L. R. Scott. *The mathematical theory of finite elements methods*, volume 15 of *Texts in Applied Mathematics*. Springer, 2002. Second edition.

[16] L. A. Caffarelli and P. E. Souganidis. A rate of convergence for monotone finite difference approximations to fully nonlinear, uniformly elliptic PDEs. *Comm. Pure Appl. Math.*, 61(1):1–17, 2008.

[17] C.-C. Chu, I. G. Graham, and T. Y. Hou. A new multiscale finite element method for high-contrast elliptic interface problems. *Math. Comp.*, 79:1915–1955, 2010.

[18] A. Doostan and H. Owhadi. A non-adapted sparse approximation of pdes with stochastic inputs. *arXiv:1006.2151*, 2010.

[19] W. E, B. Engquist, X. Li, W. Ren, and E. Vanden-Eijnden. Heterogeneous multiscale methods: a review. *Commun. Comput. Phys.*, 2(3):367–450, 2007.

[20] Y. Efendiev, J. Galvis, and X. Wu. Multiscale finite element and domain decomposition methods for high-contrast problems using local spectral basis functions. 2009. Submitted.

[21] Y. Efendiev, V. Ginting, T. Hou, and R. Ewing. Accurate multiscale finite element methods for two-phase flow simulations. *J. Comput. Phys.*, 220(1):155–174, 2006.

[22] Y. Efendiev and T. Hou. Multiscale finite element methods for porous media flows and their applications. *Appl. Numer. Math.*, 57(5-7):577–596, 2007.

[23] B. Engquist, H. Holst, and O. Runborg. Multi-scale methods for wave propagation in heterogeneous media. *To appear in Commun. Math. Sci.*, 2010.

[24] B. Engquist and P. E. Souganidis. Asymptotic and numerical homogenization. *Acta Numerica*, 17:147–190, 2008.

[25] B. Engquist and L. Ying. Sweeping preconditioner for the helmholtz equation: Hierarchical matrix representation. *Submitted*, 2010.

[26] B. Engquist and L. Ying. Sweeping preconditioner for the helmholtz equation: Moving perfectly matched layers. *Submitted*, 2010.

[27] E. De Giorgi. Sulla convergenza di alcune successioni di integrali del tipo dell'aera. *Rendi Conti di Mat.*, 8:277–294, 1975.

[28] E. De Giorgi. New problems in Γ-convergence and G-convergence. In *Free boundary problems, Vol. II (Pavia, 1979)*, pages 183–194. Ist. Naz. Alta Mat. Francesco Severi, Rome, 1980.

[29] A. Gloria. Analytical framework for the numerical homogenization of elliptic monotone operators and quasiconvex energies. *SIAM MMS*, 5(3):996–1043, 2006.

[30] A. Gloria. Reduction of the resonance error. part 1: Approximation of homogenized coefficients. *To appear in M3AS*, 2010. HAL: inria-00457159, version 1.

[31] A. Gloria and F. Otto. An optimal error estimate in stochastic homogenization of discrete elliptic equations. *To appear*, 2010. HAL: inria-00457020, version 1.

[32] H. Harbrecht, R. Schneider, and C. Schwab. Sparse second moment analysis for elliptic problems in stochastic domains. *Numer. Math.*, 109(3):385–414, 2008.

[33] Klaus Höllig. *Finite element methods with B-splines*, volume 26 of *Frontiers in Applied Mathematics*. Society for Industrial and Applied Mathematics (SIAM), Philadelphia, PA, 2003.

[34] Klaus Höllig, Ulrich Reif, and Joachim Wipper. Weighted extended B-spline approximation of Dirichlet problems. *SIAM J. Numer. Anal.*, 39(2):442–462 (electronic), 2001.

[35] T. Y. Hou and X.-H. Wu. A multiscale finite element method for elliptic problems in composite materials and porous media. *J. Comput. Phys.*, 134(1):169–189, 1997.

[36] T. Y. Hou, X.-H. Wu, and Z. Cai. Convergence of a multiscale finite element method for elliptic problems with rapidly oscillating coefficients. *Math. Comp.*, 68(227):913–943, 1999.

[37] S. M. Kozlov. The averaging of random operators. *Mat. Sb. (N.S.)*, 109(151)(2):188–202, 327, 1979.

[38] J. M. Melenk. On n-widths for elliptic problems. *J. Math. Anal. Appl.*, 247(1):272–289, 2000.

[39] Pingbing Ming and Xingye Yue. Numerical methods for multiscale elliptic problems. *J. Comput. Phys.*, 214(1):421–445, 2006.

[40] F. Murat. Compacité par compensation. *Ann. Scuola Norm. Sup. Pisa Cl. Sci. (4)*, 5(3):489–507, 1978.

[41] F. Murat and L. Tartar. H-convergence. *Séminaire d'Analyse Fonctionnelle et Numérique de l'Université d'Alger*, 1978.

[42] J. Nolen, G. Papanicolaou, and O. Pironneau. A framework for adaptive multiscale methods for elliptic problems. *Multiscale Model. Simul.*, 7(1):171–196, 2008.

[43] H. Owhadi and L. Zhang. Metric-based upscaling. *Comm. Pure Appl. Math.*, 60(5):675–723, 2007.

[44] H. Owhadi and L. Zhang. Homogenization of parabolic equations with a continuum of space and time scales. *SIAM J. Numer. Anal.*, 46(1):1–36, 2007/08.

[45] H. Owhadi and L. Zhang. Homogenization of the acoustic wave equation with a continuum of scales. *Computer Methods in Applied Mechanics and Engineering*, 198(2-4):97–406, 2008. Arxiv math.NA/0604380.

[46] G. C. Papanicolaou and S. R. S. Varadhan. Boundary value problems with rapidly oscillating random coefficients. In *Random fields, Vol. I, II (Esztergom, 1979)*, volume 27 of *Colloq. Math. Soc. János Bolyai*, pages 835–873. North-Holland, Amsterdam, 1981.

[47] A. Pinkus. *n-Width in Approximation Theory.* Springer, New York, 1985.

[48] Allan Pinkus. *n-widths in approximation theory*, volume 7 of *Ergebnisse der Mathematik und ihrer Grenzgebiete (3) [Results in Mathematics and Related Areas (3)]*. Springer-Verlag, Berlin, 1985.

[49] S. Spagnolo. Sulla convergenza di soluzioni di equazioni paraboliche ed ellittiche. *Ann. Scuola Norm. Sup. Pisa (3) 22 (1968), 571-597; errata, ibid. (3)*, 22:673, 1968.

[50] S. Spagnolo. Convergence in energy for elliptic operators. In *Numerical solution of partial differential equations, III (Proc. Third Sympos. (SYNSPADE), Univ. Maryland, College Park, Md., 1975)*, pages 469–498. Academic Press, New York, 1976.

[51] R. A. Todor and C. Schwab. Convergence rates for sparse chaos approximations of elliptic problems with stochastic coefficients. *IMA J. Numer. Anal.*, 27(2):232–261, 2007.

[52] C. D. White and R. N. Horne. Computing absolute transmissibility in the presence of finescale heterogeneity. *SPE Symposium on Reservoir Simulation*, page 16011, 1987.

[53] X. H. Wu, Y. Efendiev, and T. Y. Hou. Analysis of upscaling absolute permeability. *Discrete Contin. Dyn. Syst. Ser. B*, 2(2):185–204, 2002.

[54] V. V. Yurinskiĭ. Averaging of symmetric diffusion in a random medium. *Sibirsk. Mat. Zh.*, 27(4):167–180, 215, 1986.